Arab J Sci Eng (2014) 39:7229–7239
DOI 10.1007/s13369-014-1281-6

RESEARCH ARTICLE - MECHANICAL ENGINEERING

Definition of the Temperature and Heat Flux in Micromilling of Hardened Steel Using the Finite Element Method

Sergio Luiz Moni Ribeiro Filho · Marcelo Oliveira Gomes · Carlos Henrique Lauro · Lincoln Cardoso Brandão

Received: 25 April 2013 / Accepted: 31 October 2013 / Published online: 5 July 2014

Abstract This paper shows the influence of the mesh size on the heat flux in the micromilling process. The definition of the heat flux was based on the inverse heat conduction method (IHCM), applying the finite element technique with the Eulerian–Lagrangian approach. The micromilling was simulated with a cutter of 0.5 mm and four mesh sizes. The input parameters were two feed rates, two cutting speeds, and two radial depths of cut. Experiments were designed to verify the more significant input parameters on the heat flux and temperature. The results demonstrated that the mesh size has great influence on the responses. The values for heat flux can vary more with the mesh size than with the cutting parameters. On the other hand, the cutting speed was the parameter with the least significance. The adjusted data using IHCM for temperature, heat flux, and the convection coefficient corresponded with the traditional values.

Keywords Micromilling · Finite element analysis · Heat flux · Temperature

S. L. M. Ribeiro Filho · M. O. Gomes · C. H. Lauro · L. C. Brandão (✉)
Department of Mechanical Engineering, Federal University of São João del Rei, Praça Frei Orlando, 170, São João del Rei, CEP 36.307-352, Brazil
e-mail: lincoln@ufsj.edu.br

S. L. M. Ribeiro Filho
e-mail: sergiolmrf@gmail.com

M. O. Gomes
e-mail: ceceu_gomes@hotmail.com

C. H. Lauro
e-mail: caiquelauro@gmail.com

الخلاصة

تبين هذه الورقة العلمية تأثير حجم الشبكة في تدفق الحرارة في عملية الطحن متناهي الصغر. وقد استند تعريف تدفق الحرارة إلى طريقة التوصيل الحراري العكسي التي تطبق تقنية العنصر المحدود مع نهج أولر-اغرانج. وتمت محاكاة الطحن متناهي الصغر مع قاطع من 0.5 ملم وأربعة أحجام شبكة. وكانت معلمات الإدخال اثنتين من سرعات التغذية ، وسرعتي قطع، واثنين من الأعماق نصف القطرية للقطع. وتم تصميم التجارب للتحقق من معلمات الإدخال الأكثر أهمية على تدفق الحرارة ودرجة الحرارة. وأظهرت النتائج أن لحجم الشبكة تأثيراً كبيراً في الاستجابات. كما أن قيم التدفق الحراري يمكن أن تتغير بشكل أكبر مع حجم الشبكة منها مع معلمات القطع. وكانت من ناحية أخرى ، سرعة القطع المعلمة الأقل أهمية. إن تعديل البيانات باستخدام طريقة التوصيل الحراري العكسي لدرجة الحرارة تدفق الحرارة ، ومعامل الحمل الحراري تتفق والقيم التقليدية.

1 Introduction

The finite element method is a good alternative to predict the temperature in the cutting zone in machining processes. This is the case because machining processes present an intricate region to measure the temperature and define the heat flux between the tool and work piece. The definition of the temperature fields in the cutting zone is complex because a part of the heat goes to the tool, another part goes to the work piece, and the largest part of the heat is removed by the chip detached from the cutting region. The most common modern technique for monitoring the temperature is the use of an embedded thermocouple. Thermocouples can be used in all machining processes and provide highly accurate information. In the last years, therefore, several authors have used thermocouples to monitor temperatures and define the heat flux in machining. The use of embedded thermocouples, for example, consists of inserting a fine wire into a hole near the cutting zone where the thermal fields are assessed. Aneiro et al. [1] monitored the temperature in a turning process applying this technique. In their case, the thermocouple was inserted into the tool,

acquiring the temperature 0.1 mm below the cutting region. The results showed that, in spite of the distance of 0.1 mm between the thermal fields and the thermocouple, the values were accurate and provided good information about the coatings and coolant fluids.

Generally, the understanding of the temperature values in a machining process is linked to another important parameter, which is the heat flux. The increase in temperature generates a great amount of heat flux in the machining process and accelerates tool wear through the diffusion mechanism. The increase in temperature is associated with the increase in cutting speed. Carbide tools and their coatings should therefore be improved to resist the increase in temperature in machining using the temperature information.

Coelho et al. [2,3] monitored the temperature and defined the heat flux and convection coefficient in drilling and tapping processes applying three different cooling systems. It is worth noting that it is difficult to monitor temperatures in tapping and drilling because the tool is always inside a hole that hinders the perfect actuation of the coolants. It is important at this point to try to understand the heat reducing capabilities of cooling systems in machining based on the information obtained from monitoring the temperature.

It is interesting to note that the use of embedded thermocouples depends on a setup that requires the work piece to be drilled to insert the thermocouple. Furthermore, a special device has to be linked to a system to guarantee the positioning of the measure system. There are, therefore, different setups to insert thermocouples that depend on the machining process. Lazard and Corvisier [4] monitored the temperature in turning using a configuration where the thermocouple was mounted near the tool's tip. The results showed that the transient temperatures found at the tip of a turning tool can avoid the damage or the breaking of the tool.

The temperature data recorded by thermocouples enable the definition of the heat flux in cutting zones using indirect mathematical methodologies. This is why the inverse heat conduction method (IHCM) can be applied to find the heat flux. Brandão et al. [5] used an inverse heat conduction technique based on Carslaw and Jaeger [6]. The proposed model uses the moving heat source theory to express the temperature reached at the interface of two semi-infinite solids in sliding contact. De Souza et al. [7] also applied the inverse technique to estimate temperature and heat flux at the tool and work piece interface during the drilling process, basing their method on Green's function. Luchesi and Coelho [8] proposed an inverse method to estimate the heat sources in the transient two-dimensional heat flux in a rectangular domain. According to the authors, all techniques employed provided the definition of the heat flux from the temperature measurement of the machining process.

Besides the use of thermocouples, the application of the thermograph is a good strategy to define temperatures in machining. Because of its ease in monitoring machining processes, an infrared camera can be used without complex preliminary setups. According to Pittalà and Monno [9], the model is consistent because it provides a good agreement between theoretical and experimental temperature. The authors also used a finite element model to define the sensitivity in the boundary conditions. Iqbal et al. [10] also modeled the dry sliding of metals to estimate the interface heat transfer coefficient. The results of the dry sliding process yield the interfacial heat transfer coefficient for a range of speeds.

The finite element technique has been widely applied to machining simulations since the development of computer technology. ANSYS^{TM} and Abaqus^{TM} are the most commonly used finite element software to evaluate temperature, cutting forces, and residual stress in the manufacturing process. It is necessary, however, to previously know the materials' input parameters, such as conductivity, diffusivity, coefficient of thermal expansion, and modulus of strain hardening. Generally, the information of the material's physical and thermal properties is defined based on experimental or simulation work. Wu and Han [11] estimated the temperature in the drilling process using the finite element method with different meshing of the work pieces. The authors support that the methodology provided a good agreement between the measured and predicted temperature.

In some cases, the use of mixed techniques can help to obtain more accurate data. Authors as Brandão et al. [12] and Umbrello et al. [13] used thermocouples and finite element to define the heat flux in milling and turning, respectively. Both authors used Chromel/Alumel thermocouples (K-Type) with an average diameter of 0.5 mm. The results showed a good match between experimental and simulation data. However, according to the authors, further consistent extensions of the numerical simulation should be performed, such as wear prediction, 3D geometry's analysis, plastic strain, and others.

Courbon et al. [14] analyzed the thermal contact conditions at the tool–chip interface. The authors studied the machining of AISI 1045 steel in two parts. The first was carried out in orthogonal cutting conditions using coated carbide tools. The second was the evaluation of how the perfect thermal contact can be inferred in the contact zone using a finite element methodology. According to the authors, the results produced data for a better understanding and definition of the tribological behavior in the chip–tool interface.

Nowadays, micro end milling is becoming an important manufacturing process. Micromachining is suited for use in applications that require specific characteristics, such as small batches and the manufacture of prototypes. Just as in macro milling, micromilling provides products with complex geometries and specific features. However, according to Wissmiller and Pfefferkorn [15], the successful application of micro end milling requires accurate parameters for tolerance, surface finish quality, and limited tool wear. The

authors studied the micromilling in 1018 steel and 6061-T6 aluminum with cutters of 300 μm. Unlike what occurs in macro milling, the thermal gradients are largest in the flute and in the transition sections because of the thermal resistance in function of the smaller cross-sectional area.

Thus, considering that cutting zone temperatures in micromachining are significantly lower than in macro milling, new studies need to be developed to improve the knowledge in micromachining. Based on these studies, it may prove desirable to reduce the temperature fields to increase the micro tools productivity. This paper presents an investigation to define the temperature in micromilling with different mesh sizes. In addition, and heat flux resulting from the heating through micromilling are also investigated using the inverse heat conduction methodology.

2 Methodology

The micromilling simulations were developed considering the AISI AISI H13 steel with different mesh sizes. The experimental monitoring of the temperature in the micromilling process is very difficult because of the size scale. In the case of macro milling, the size of the cold joint of the thermocouple is smaller than the size of the cutter. In micromilling, on the other hand, the cold joint can be bigger than the diameter of the tool. Considering the difficulty in measuring the temperature with thermocouples, the aim this work was to acquire the temperatures for micromilling using simulation tests according to the variation of the cutting parameters.

Afterward, the temperature curves were adjusted to define the heat flux based on a specific mathematical model. The simulations were performed with four mesh sizes: 50, 100, 250, and 400 μm. For each mesh size eight simulations with two cutting speeds (V_c), two feed rates (f), and two radial depths of cut (a_e) were carried out, as shown in Table 1. The axial depth of cut (a_p) was considered as a constant value due to its small influence in the milling process and a transient simulation with a total time at 120 s and steps of 0.04 s was chosen.

Considering the finite element problems, the mesh size has a great influence on the computational time and final solution. Different mesh sizes are usually tested for the adjustment and accuracy of the results. In this article, several mesh sizes are used to define the effect of mesh on heat flux in the analytical model. Given that the monitoring of the experimental values is very difficult, the accuracy of the results is validated by adjusting the values between the finite element models and the model proposed by Carslaw and Jaeger [6].

The micromilling process was simulated considering a dynamic thermomechanical finite element using an explicit integration. The chip formation during micro cutting was simulated with a strain gradient based on FE models. A more

Table 1 Cutting parameters used in simulations

Simulation number	Cutting speed Vc (m/min)	Feed rate f_Z (mm/rot)	Radial depth of cut a_e (mm)
1	77	0.08	0.50
2	77	0.08	0.25
3	77	0.03	0.50
4	77	0.03	0.25
5	47	0.08	0.50
6	47	0.08	0.25
7	47	0.03	0.50
8	47	0.03	0.25

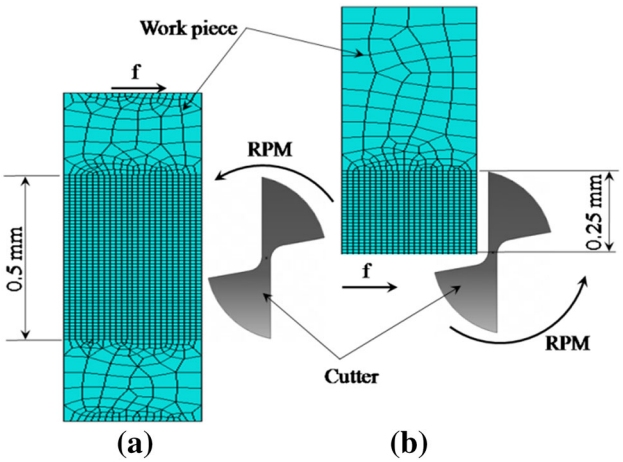

Fig. 1 Models used in simulation in plane x–y; **a** radial depth of cut of 0.5 mm, **b** radial depth of cut of 0.25 mm

detailed description for the strain gradient plasticity model can be found in the work of Liu and Melkote [18] and Lai et al. [19]. The friction coefficient in the cutting region between tool and work pieces was 0.1, according to [20].

The tool was modeled considering an isothermal rigid body. The tool was based on the micro cutter code R216.32-00530-AE05G 1620 produced by SANDVIK Coromant™ [21]. The meshes used in the cutting region of the work pieces were parametric elements with four nodes and mesh sizes ranging from 50 to 400 micrometers. Asymmetrical elements were used in order to decrease the simulation time. The top and bottom of the work piece were therefore not affected by the cutting process. The simulations were carried out taking into account only the micromilling in dry conditions. The generated mesh used the CPE4R element with four nodes by element and elements with square shape. Figure 1 shows the 3D model of the work piece with 1.2 mm of width and the tool with 0.5 mm of diameter. Tables 2, 3 and 4 exhibit the Johnson–Cook plasticity model applied to the hardened AISI AISI H13 steel with 49 HRC, according to [16,22].

Table 2 Johnson Cook's constants [23]

A—Initial Von Mises Stress (MPa)	715
B—Modulus of strain hardening (MPa)	329
C—Strain rate sensitivity	0.03
m—Coefficient of thermal expansion	1.13
n—Cold work rate	1.5

Table 3 Johnson Cook's parameter [16]

D1—Johnson Cook's parameter	−0.8
D2—Johnson Cook's parameter	2.11
D3—Johnson Cook's parameter	−0.5
D4—Johnson Cook's parameter	0.0002
D5—Johnson Cook's parameter	0.61

Table 4 Parameters of the material (AISI H13) [22]

Specific heat (J/kg K)	560
Coefficient of thermal expansion (N/s/mm/C)	40
Thermal conductivity (W/m K)	37
Density (kg/m^3)	7,800
Young's modulus (GPa)	211
Poisson's ratio	0.28

The simulation was divided into two models using upward milling, which provides the worst milling conditions and highest temperature values. The first model was based on micromilling with an axial depth of cut (a_p) of 0.05 mm and radial depth of cut (a_e) of 0.5 mm, according to Fig. 1a. The second model used the same axial depth of cut, but the radial depth of cut was 0.25 mm, as shown in Fig. 1b. Room temperature was used for the work piece as an initial condition. Micromilling can be assumed to be an adiabatic process, since the cutting speed is very high and the micro cutting process is performed for a short period of time. The finite element analysis was therefore carried out considering only conduction and neglecting convection and radiation. In metal cutting, the heat is generated by plastic deformation of the material and the friction between two surfaces in contact [22]. The inelastic heat fraction used in the model was similar to other researchers [23]. In addition, the heat generation due to the contact between chip–tool specimen interfaces was considered.

The nodes of surface (a) and (b) are constrained in the *x*–*y*–*z* plane, as shown in Fig. 1. The displacement of the tool was considered only in the cutting direction. The rotation and the linear movement of the tool were constrained at the reference point (RP). Different cutting speeds were implemented at the RP in the cutting direction, according to Table 1. Figure 2 shows the deformed work piece and the location where the temperature was measured.

3 Analysis of Results

3.1 Theoretical and Simulation Evaluation

The heat source theory was adopted to calculate the temperature of a one-dimensional moving point. The one-dimen-

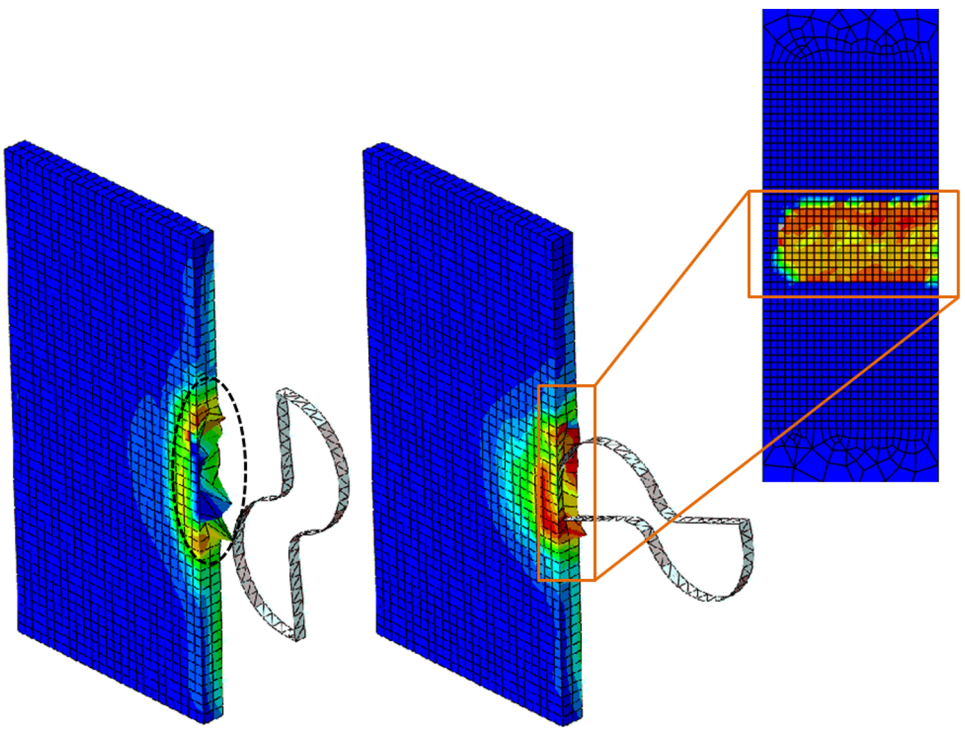

Fig. 2 Deformed work piece and the location where the temperature was measured

sional model was considered due to the small dimensions of the radial and axial depth of cut. The diameter of the tool can be analyzed as a point that moves through the material and generates heat. Thus, the heat source will move as a point source in a line that loses heat by convection, according to Fig. 3. Based on this, the energy balance can be written according to Eq. (1).

$$q_x + q_{x+\mathrm{d}x} = \Delta U \tag{1}$$

where q_X input heat energy from conduction [J]; ΔU internal energy [J].

However, in this work, the cooling systems were not considered, and the simulation was carried out only in dry conditions. This can be justified because the micromilling process does not use cooling systems. The small size of the cutter gives it low resistance to the high pressure of cooling systems. Thus, the size of chips is smaller and their removal is not required from the cutting region applying high-pressure jets. Just as occurs in macro milling, the heat source is the result of chip formation plus the friction of the tool on the material during the milling. There is a heat flux in the radial direction, but because of the high speed in the micromilling the heat flux takes longer to spread, and it was not considered.

Considering the diffusivity of the material "α", which is a constant that depends on the density "ρ", of the material's specific heat "c_p", and the milled area "$A_c = ae{*}ap$". Equation (1) can be rewritten using Fourier's model, as demonstrated in Carl and Jaeger [6], and the final result shown in Eq. (2). Thus, the model proposed and developed by Carslaw and Jaeger [6], and used by Brandão et al. [5] in the drilling process, can also be applied in this analysis. However, the proposed model was adapted for this simulation disregarding the cooling system. Thus, the model considers only the maximum values at the "x" point and the velocity of displacement of the heat source "v".

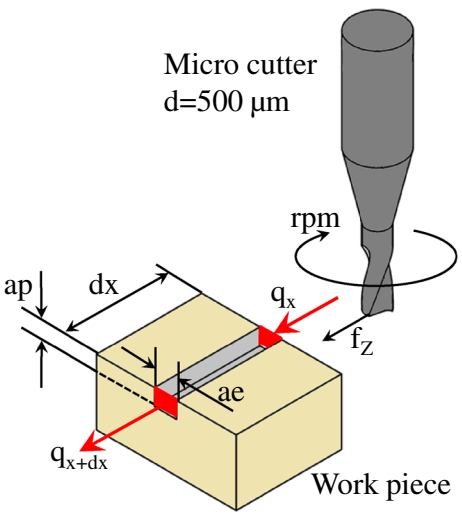

Fig. 3 Schematic of the system

$$\theta = \frac{q}{2 \cdot A_c \cdot \rho \cdot c_p (\pi \cdot \alpha \cdot t)^{\frac{1}{2}}} e^{-\left(\frac{x - v \cdot t}{4 \cdot \alpha \cdot t}\right)} \tag{2}$$

where q heat flux [W];

Equation (2) gives the temperature at a certain point, "x", as a function of time, due to a moving heat source along the "x" axis. Thus, a system can be placed at point "x" to record the temperature and to register the temperature-time curve, adjusting it to Eq. (2). Based on this, the simulation tests were carried out according to the data of Table 1. The results were temperature curves that vary according to the milling conditions. The temperature peaks were analyzed with the Abaqus' software considering a measurement point positioned at the node between the first and second element. This point represented, for example, the position where a thermocouple was inserted. Thus, a transient simulation was performed with a total time at 120 s performed with steps of 0.04 s.

3.2 Temperature Measurement and Heat Flux Definition

The aim of this work was to find the heat flux and temperatures values using the inverse heat conduction methodology (IHCM). The fitting was carried out only for dry micromilling system for all cutting conditions. The Abaqus software generated a temperature values matrix that was saved in a "txt" file and the fitting was performed using the MatLab™ software. A routine was developed to analyze the temperature data from Abaqus™ and find the values for heat flux "q". As shown in Fig. 4, the temperature stabilized in 0.01 s, and it was constant until the end of simulation. The red line represents the results of the simulated temperature and the blue line the fitted temperature, according to the model proposed by Eq. 2. The fitting in Fig. 4 was generated with the small mesh size of 50 µm proposed in this work. On the other hand, Fig. 5 represents the fitting for the greatest mesh size of 400 µm. As can be observed in Figs. 4 and 5, there is a difference between the fitting of the mathematical and simulation models. This difference may be explained by the considered heat transfer model. The simulation uses Fourier's law for the fitting of the temperature according to physical and thermal parameters. The behavior of temperature in both the mathematical and simulation tests can be considered to be similar. A quick increase in temperature occurred, but this depends on the mesh size, a great difference in the adjustment occurs after the maximum temperature peak of for the mesh size of 50 µm. The mesh size of 400 µm showed the best adjustment of temperature, demonstrating that Fourier's model applied to the mathematical model provides good information about heat flux because the difference between the mathematical model and simulation was smaller. The peak value of the temperature was 500 °C for the mesh size of 50 µm, which

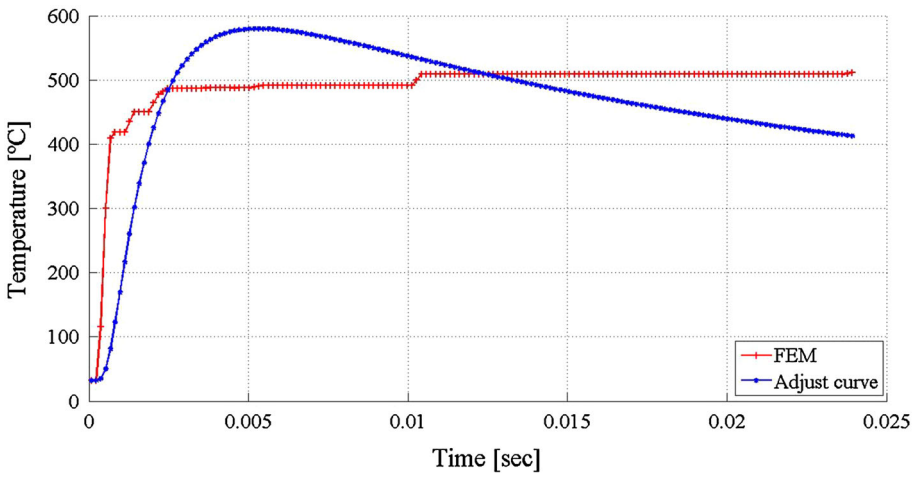

Fig. 4 Temperature curves for mesh sizes of 50 μm (V_c = 47 m/min, f = 0.03 mm/rot, and a_e = 0.25 mm)

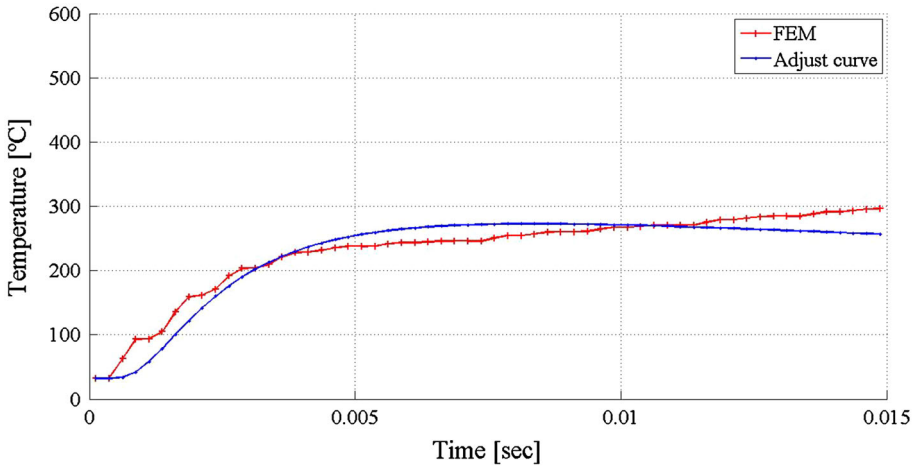

Fig. 5 Temperature curves for the mesh size of 400 μm (V_c = 47 m/min, f = 0.03 mm/rot, and a_e = 0.25 mm)

Table 5 Parameters used in simulation

Symbols	Cutting parameters	Simulation levels
Vc	Cutting speed (m/min)	47 77
f	Feed rate (mm/rot)	0.030 0.080
ae	Radial depth of cutting (mm)	0.25 0.50
Mesh	Mesh size (microns)	50 100 250 400

can be considered very high for this type of machining considering the references.

As can be seen in Fig. 5, the fitting was closer for the mesh size of 400 μm, considering the same cutting conditions. The behavior of the simulated temperature curve is different for the mesh size of 50 μm, not showing a quick increase until the maximum peak. First, the temperature increases until 225 °C in 0.005 s and afterward it increases at a slower rate until it reaches the maximum value of 360 °C. The total time to reach the peak was 0.015 s being a time slower than the mesh size of 50 μm.

The temperature peak for the mesh size of 50 μm occurred first for the simulation test and later for the mathematical model. On the other hand, the temperature for mesh size of 400 μm tended to increase steadily. It demonstrates that the perfect fitting to define the heat flux depends on the mesh size. It can therefore be supported that the use of both models simultaneously is very important because one confirms the data generated by the other.

3.3 Statistical Analysis

Table 5 shows the main parameters used in the simulation with their respective levels. The levels for cutting speed, feed rate, and depth of cut were chosen based on the information of the tool's supplier. The mesh size was defined considering the equivalent proportion used by Lauro [17] who carried out experimental micromilling tests with grain sizes of 39 and

Table 6 Results for temperature and heat flow "q" (full factorial design $2^3 4^1$)

Simulation number	Cutting speed (m/min)	Feed rate (mm/rot)	Depth of cut (mm)	Mesh size (μm)	Temperature (°C)	Heat flux (W)
1	77	0.03	0.25	400	347.951	1.1532
2	47	0.03	0.25	50	510.983	1.3173
3	77	0.03	0.50	50	553.189	1.6574
4	77	0.03	0.25	250	403.097	1.2158
5	47	0.03	0.50	100	509.738	1.7170
7	47	0.03	0.50	400	399.792	1.1451
8	47	0.08	0.50	250	437.119	1.4789
9	77	0.03	0.50	400	415.667	1.5287
10	77	0.08	0.25	100	496.069	1.5017
11	47	0.08	0.25	250	435.020	1.2999
12	77	0.08	0.50	50	547.083	1.3304
13	77	0.03	0.50	100	511.274	1.5573
14	77	0.08	0.25	50	878.070	3.6548
15	47	0.08	0.25	400	341.330	1.3709
16	77	0.08	0.25	400	343.788	1.1208
17	47	0.03	0.50	250	429.162	1.4036
18	47	0.03	0.50	50	509.738	1.7170
19	47	0.08	0.50	100	500.232	1.6915
20	47	0.03	0.25	400	341.978	1.4070
21	77	0.08	0.50	100	529.544	1.5447
22	77	0.08	0.50	250	440.035	1.4412
23	47	0.03	0.25	100	506.788	1.7212
24	47	0.08	0.25	100	494.397	1.6727
25	47	0.03	0.25	250	370.499	1.4986
26	77	0.08	0.50	400	400.971	1.3302
27	77	0.03	0.25	50	878.070	3.2928
28	47	0.08	0.25	50	818.510	3.4640
29	77	0.03	0.50	250	447.912	1.4279
30	77	0.03	0.25	100	495.909	1.6204
31	47	0.08	0.50	400	385.923	1.1216
32	77	0.08	0.25	250	435.020	1.2999

497 μm. The same tool geometry, cutting speed, feed rate, and depth of cut were also applied in simulation tests.

Table 6 shows all results obtained from simulation for the temperature and heat flux responses. The temperature ranged from 347.951 to 878.070 °C, and it can be noted that the value of 878.070 °C was the same for the experiments number 14 and 27, but a variation of the feed rate can be observed. The heat flux ranged from 1.1208 to 3.6548 W. However, identical values for heat flux were not found as this occurred for temperature. It is important to understand that the simulation tests are significant for finding the best responses for a specific process. A previous understanding, however, of a range of simulated values or further evidence proving the data using experimental tests after the simulation is necessary. Considering, therefore, that the mean Torque found by Lauro [17] with the same input cutting parameters and work piece material was 0.0165 N m, the energy "P" in Watts of the process can be calculated according to Eq. (3).

$$P = \frac{2 \cdot \pi \cdot N}{60} T \tag{3}$$

where "N" is the spindle speed of the high-speed machining head and "T" the mean torque generated in micromilling. The lowest energy was 11.0 W and the highest was 35.9 W, corresponding to a range of 4–12 % of the total energy supplied during the micromilling process. Based on this, the theoretical values for "q" were in accordance with the values defined by Woon et al. [20]. The author supports that the heat flux that goes to the work piece is near to 10 % of the cutting power of macro machining processes.

4 Analysis of Variance for Taguchi Design

The analysis of variance (ANOVA) was carried out to verify if the main and/or the interaction factors are statistically significant with a 95 % confidence interval. The "*F*" coefficient represents the ratio of the adjusted mean square of each factor by the average square error. The *P* values indicate which of the effects throughout the system are statistically significant, based on an the orthogonal array considered in this study to analyze the effects. The orthogonal array is based on the Taguchi technique. The temperature values determined by numerical tests for both situations were denominated as replicate 1 in the Taguchi design. The Taguchi method enables the drastic reduction of the number of tests with no replicates. The effect is considered significant when the *P* value is less than or equal to 0.05. A α-level of 0.05 is the level of significance, which implies that there is 95 % of probability of the effect being significant. Moreover, the results are presented via main effect and interaction plots. Table 7 shows a summary of *P* values for Temperature and Heat Flux.

Larger values for R^2 suggest that the Temperature and Heat Flux models are a good fit with the data. Furthermore, there was strong evidence for a significant effect of the cutting speed on the response temperature. It is interesting to note that, the same way this occurs in macro machining, the cutting speed has a significant influence on temperature. Despite of the dimension of the cutter, the temperature data for all simulation tests varied from 341.33 to 878.070 °C. The mesh size also proved to have a significant effect on temperature and heat flux. It can therefore be supported that the results can vary significantly depending on the defined mesh size in temperature simulation tests.

4.1 Response Surface Methodology

The RSM method generates a second-order model that demonstrates the second-order effect of each input parameter separately and the two-way interaction between combinations of these parameters. Thus, the second-order mathematical model can be represented according to Eq. (4).

$$Y = b_0 + \sum_{i=1}^{n} b_i x_i + \sum_{i=1}^{n} b_{ii} x_i^2 + \sum_{i<j}^{n} b_{ij} x_i x_j + \varepsilon \tag{4}$$

where b_0 represents the linear effect of x_i; b_{ii} represents the quadratic effect of x_i; b_{ij} shows the linear-by-linear interaction between x_i and x_j

Table 7 Analysis of variance for temperature, heat flux "*q*", *P* values ($\alpha \leq 0.05$)

Sources	Temperature (°C)		Heat flux (W)	
	F	*P*	*F*	*P*
Cutting speed	8.38	***0.021***	0.020	0.891
Feed rate	1.75	0.198	0.880	0.357
Radial depth of cut	0.27	0.610	1.110	0.303
Mesh size	19.22	***0.000***	7.940	***0.001***
Cutting speed * feed rate	0.58	0.248	1.843	0.843
Cutting speed * radial depth of cut	3.75	0.452	7.090	0.739
Cutting speed * mesh size	0.57	0.981	6.770	0.770
Feed rate * radial depth of cut	1.22	0.520	2.380	0.387
Feed rate * mesh size	0.38	0.335	4.150	0.750
Radial depth of cut * mesh size	0.75	0.411	2.610	0.610
Cutting speed * feed rate * radial depth of cut	0.77	0.470	3.843	0.843
Cutting speed * feed rate * mesh size	3.72	0.706	1.739	0.639
Cutting speed * radial depth of cut * mesh size	4.68	0.651	7.800	0.730
Feed rate * radial depth of cut * mesh size	14.12	0.720	2.740	0.388
Cutting speed * feed rate * radial depth of cut * mesh size	4.63	0.841	4.150	0.253
R^2(adj)	80.60 %		81.5 %	

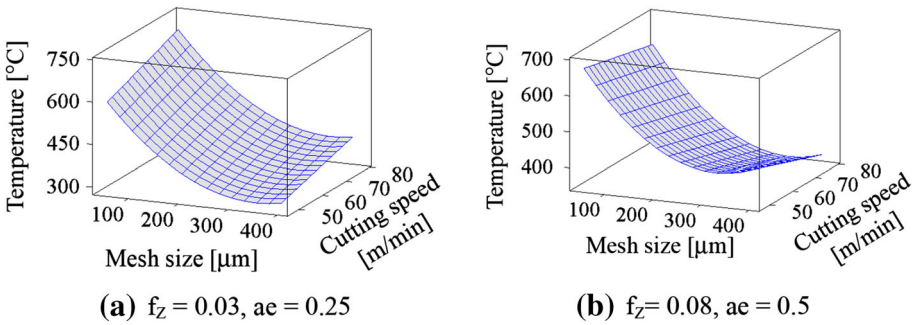

Fig. 6 Response surfaces for temperature

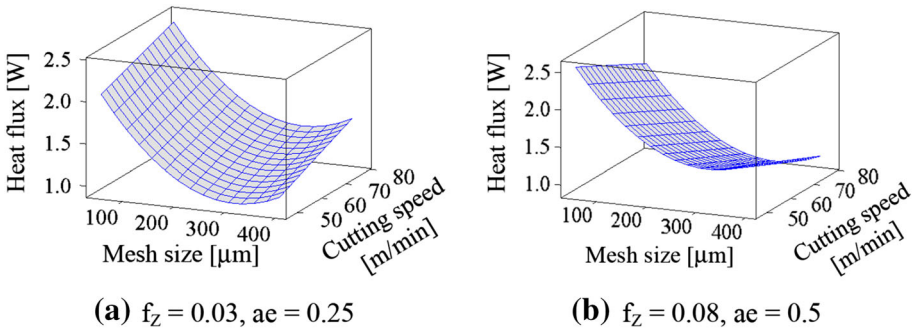

Fig. 7 Response surfaces for heat flux

Table 8 Analysis of variance for temperature (°C) and heat flux (W)

Source	Heat flux		Temperature	
	F	*P*	*F*	*P*
Regression	2.42	***0.041***	5.43	***0.001***
Linear	3.90	***0.017***	10.91	***0.000***
Square	4.09	0.057	6.54	***0.019***
Interaction	1.00	0.453	1.44	0.249

In addition, Central Composite Design was applied to establish a correlation between the feed rate and radial depth of cut on temperature and heat flux. Figure 6a shows that the RSM for temperature varied from 300 to 750 °C considering the feed rate (f_Z) of 0.03 mm/rev and radial depth of cut (ae) of 0.25 mm. Figure 6b shows that the RSM for temperature varied from 400 to 700 °C considering the feed rate (f_Z) of 0.08 mm/rev and radial depth of cut (ae) of 0.5 mm. The variation of the temperature value is based on the feed rate (f_Z) and radial depth of cut (ae) parameters. According to Fig. 6a, b, the RSM has a curve behavior in the mesh size axis and a linear behavior in the cutting speed axis. It can therefore be observed that the temperature increases with the decrease in mesh size. Thus, the mesh size had influence on temperature due to the dimension of the parametric element used in simulation that varied proportionally to the mesh size. Small mesh sizes accumulate more heat than great mesh sizes avoiding the quick cooling between the borders of the elements. Moreover, the curve increases for mesh sizes larger than 400 µm, showing an ideal point for the mesh size situated between 300 and 400 µm.

In the opposite situation, the increase in temperature considering the cutting speed (Vc) is almost constant with a small inclination. However, the temperature increases for the input parameters $f_Z = 0.03$ mm/rot and $ae = 0.25$ mm and decreases for the input parameters $f_Z = 0.08$ mm/rot and $ae = 0.5$ mm. It can therefore be supported that the simultaneous use of a small feed rate and radial depth of cut increases the temperature when the cutting speed increases. On the other hand, the use of a large feed rate and radial depth of cut decreases the temperature with the increase in cutting speed. The use of large input parameters provides the best removal of the heat flux in the milling process and, consequently, a lower temperature. This situation can be confirmed in Fig. 7a, b, which show a similar behavior for temperature. The temperature is strongly related to heat flux. The two responses work together and they have a directly proportional behavior. The heat flux results varied from 1.0 to 2.5 W.

The RSM model can be used to predict the temperature and heat flux. Table 6 shows the analysis of variance for temperature taking into account the simulation tests. According to Table 8, the regression linear and the square models have influence on the temperature, but only the regression and linear model have influence on heat flux. As mentioned previously, the α-level of 0.05 is the level of significance that implies that there is 95 % of probability of the effect being significant. Thus, the values of 0.001, 0.000, and 0.019 for the P value are significant for the temperature response. In the same way, the values of 0.041 and 0.017 are significant for the heat flux. It demonstrates that the three models can

be used to predict the temperature within a specific limit. In the same way, only the regression and linear models can be used to predict the heat flux. On the other hand, the interaction among models (regression, linear, and square) do not influence the temperature and heat flux responses.

The temperature of the milled work piece can therefore be expressed as a function of input factors, such as feed rate, radial depth of cut, cutting speed, and mesh size. Equation (6) shows the mathematical model to define the temperature value and Eq. (7) shows the mathematical model to define the heat flux value.

$$\begin{aligned}\text{Temp}\,(^{\circ}\text{C}) &= 306.965 + 7.80769^{*}Vc + 5{,}747.77^{*}f_Z \\ &\quad + 231.448^{*}ae - 2.52159^{*}\text{Mesh} + 0.0033647^{*}\text{Mesh}^2 \\ &\quad - 52.9043^{*}Vc^{*}f_Z - 10.0501^{*}Vc^{*}ae \\ &\quad - 0.0023756^{*}Vc^{*}\text{Mesh} - 1{,}039.84^{*}f_Z^{*}ae \\ &\quad - 6.20208^{*}f_Z^{*}\text{Mesh} + 191{,}727^{*}ae^{*}\text{Mesh} \qquad (6)\end{aligned}$$

$$\begin{aligned}Q &= 0.673396 - 0.0335211^{*}Vc + 36.0241^{*}f_Z \\ &\quad - 1.34342^{*}ae - 0.011285^{*}\text{Mesh} + 0.0000166^{*}\text{Mesh}^2 \\ &\quad - 0.322223^{*}Vc^{*}f_Z - 0.0504813^{*}Vc^{*}ae \\ &\quad + 0.0000072^{*}Vc^{*}\text{Mesh} - 9.09758^{*}f_Z^{*}ae \\ &\quad - 0.041881^{*}f_Z^{*}\text{Mesh} + 0.0076158^{*}ae^{*}\text{Mesh} \qquad (7)\end{aligned}$$

5 Conclusions

The thermo effect of the micromilling of hardened AISI H13 steel was assessed through finite element analysis. The FE model was carried out based on numerical approaches because of the difficulty of predicting the complete damage mechanism of micro cutting processes experimentally. A finite element model of micromilling cutting was successfully developed to predict the relationship between temperature and heat flux with different cutting speeds, axial depths of cut, radial depths of cut, and mesh sizes for the analytical models. The temperature and heat flux parameters were chosen because they are directly proportional and represent the most accurate information for the tools design. The results showed that the analysis of variance was able to define which input parameters were of influence on the responses. The combined application of a simulation and the IHCM showed that the mesh size was the significant input parameter. The use of RSM generated a mathematical model that was capable of predicting the temperature and heat flux. The model also supported that the best size mesh laid between the 300 and 400 μm. The values for the heat flux were approximately 10 % of the total power generated in the micromilling process.

References

1. Aneiro, F.M.; Coelho, R.T.; Brandão, L.C.: Turning hardened steel using coated carbide at high cutting speeds. J. Braz. Soc. Mech. Sci. Eng. **30**(2), 104–109 (2008)
2. Coelho, R.T.; Brandão, L.C.; Malavolta, A.T.: Experimental and theoretical study on work piece temperature when tapping hardened AISI AISI H13 using different cooling systems. J. Braz. Soc. Mech. Sci. Eng. **32**(2), 154–159 (2010)
3. Coelho, R.T.; Brandão, L.C.: Temperature and heat flux when tapping of the hardened Steel using different cooling systems. Ingeniare Revista Chilena de Ingeniería **17**(2), 267–274 (2009)
4. Lazard, M.; Corvisier, P.: Modeling of a tool during turning Analytical prediction of the temperature and of the heat flux at the tool's tip. Appl. Therm. Eng. **24**, 839–849 (2004)
5. Brandão, L.C.; Coelho, R.T.; Lauro, C.H.: Contribution to dynamic characteristics of the cutting temperature in the drilling process considering one dimension heat flux. Appl. Therm. Eng. **31**, 3806–3813 (2011)
6. Carslaw, H.S.; Jaeger, J.C.: Conduction of Heat in Solids, 2nd edn, p. 510. Oxford, London (1985)
7. de Sousa, P.F.B.; Borges, V.L.; Pereira, I.C.; da Silva, M.B.; Guimarães, G.: Estimation of heat flux and temperature field during drilling process using dynamic observers based on Green's function. Appl. Therm. Eng. **48**, 144–154 (2012)
8. Luchesi, V.; Coelho, R.Y.: An inverse method to estimate the moving heat source in machining process. Appl. Therm. Eng. **45-46**, 64–78 (2012)
9. Pittalà, G.M.; Monno, M.: A new approach to the prediction of temperature of the workpiece of face milling operations of Ti–6Al–4V. Appl. Therm. Eng. **31**, 173–180 (2011)
10. Iqbal, S.A.; Mativenga, P.T.; Sheikh, M.A.: An investigative study of the interface heat transfer coefficient for FE modeling of high speed machining. NED Univ. J. Res. **4/1**, 44–58 (2009)
11. Wu, J.; Han, R.D.: A new approach to predicting the maximum temperature in dry drilling based on a finite element model. J. Manuf. Process. **11**, 19–30 (2009)
12. Brandão, L.C.; Coelho, R.T.; Rodrigues, A.R.: Experimental and theoretical study of work piece temperature when end milling hardened steels using (TiAl)N-coated and PcBN-tipped tools. J. Mater. Process. Technol. **199**(1 e 3), 234–244 (2008)
13. Umbrello, D.; Filice, L.; Rizzuti, S.; Micari, F.; Settineri, L.: On the effectiveness of finite Element simulation of orthogonal cutting with particular reference to temperature prediction. J. Mater. Process. Technol. **189**, 284–291 (2007)
14. Courbon, C.; Mabrouki, T.; Rech, J.; Mazuyer, D.; D'Eramo, E.: On the existence of a thermal contact resistance at the tool-chip interface in dry cutting of AISI 1045: formation mechanisms and influence on the cutting process. Appl. Therm. Eng. **50/1**, 1311–1325 (2013)
15. Wissmiller, D.L.; Pfefferkorn, F.E.: Micro end mill tool temperature measurement and prediction. J. Manuf. Process. **11**, 45–53 (2009)
16. Ng, E.; Aspinwall, D.K.: Modelling of hard part machining. J. Mater. Process. Technol. **127**, 222–229 (2002)
17. Lauro, C.H.: Numerical Analysis with Experimental Validation of Cutting Forces in Micromilling Process of Hardened Steels with Variation of Austenitic Grain Sizes, M.Sc. Thesis, Federal University of São João del Rei, 82 p. (in Portuguese)
18. Liu, K.; Melkote, S.N.: Finite element analysis of the influence of tool edge radius on size effect in orthogonal micro-cutting process. Int. J. Mech. Sci. **49**, 650–660 (2007)

19. Lai, X.; Li, H.; Lin, Z.; Ni, J.: Modeling and analysis of micro scale Milling considering size effect, micro cutter edge radius and minimum chip thickness. Int. J. Mach. Tools Manuf. **48**, 1–14 (2008)
20. Woon, K.S.; Rahman, M.; Fang, F.Z.; Neo, K.S.; Liu, K.: Investigations of tool edge radius effect in micromachining: a FEM simulation approach. J. Mater. Process. Technol. **167**, 316–337 (2007)
21. SANDVIK: "Catálogo de produtos", 490 p. (in Portuguese) (2012)
22. Chen, L.; El-Wardany, T.I.; Nasr, M.; Elbestawi, M.A.: Effects of edge preparation and feed when hard turning a hot work die steel with polycrystalline cubic boron nitride tools. CIRP Ann. Manuf. Technol. **55**, 89–92 (2006)
23. Longère, P.; Dragon, A.: Evaluation of the inelastic heat fraction in the context of microstructure-supported dynamic plasticity modelling. Int. J. Impact Eng. **35**, 995–999 (2008)